Vacuum 152 (2018) 200–204

Contents lists available at ScienceDirect

Vacuum

journal homepage: www.elsevier.com/locate/vacuum

Short communication

Porous germanium formed by low energy high dose Ag^+-ion implantation

A.L. Stepanov [a, b, c, *], V.I. Nuzhdin [a], V.F. Valeev [a], A.M. Rogov [b], V.V. Vorobev [b], Y.N. Osin [b]

[a] Kazan Physical-Technical Institute, Russian Academy of Sciences, 420029, Kazan, Russia
[b] Kazan Federal University, 420008, Kazan, Russia
[c] Kazan National Research Technological University, 420015, Kazan, Russia

A R T I C L E I N F O

Article history:
Received 18 February 2018
Accepted 19 March 2018
Available online 21 March 2018

Keywords:
Porous germanium
ion implantation
Silver nanoparticles

A B S T R A C T

A technical approach is proposed for the synthesis of thin porous PGe layers with Ag nanoparticles based on low-energy high-dose implantation of single-crystal *c*-Ge metal ions. To demonstrate a successes of this techniqe, we performed an Ag^+-ion implantation of a polished *c*-Ge substrates with an energy of 30 keV at a dose of $1.5 \cdot 10^{17}$ ion/cm^2 and a current density of 5 μA/cm^2. Methods of scanning electron and atomic force microscopy, as well as EDX analysis and electron backscattered diffraction was shown that as a result of the implantation on the c-Ge surface a porous amorphous PGe layer is formed of a spongy structure consisting of a network of intersecting Ge nanowires with an average diameter of ~10–20 nm. At the ends of the nanowires, the synthesis of Ag nanoparticles is observed. It was found that the formation of pores during Ag^+-ion implantation is accompanied by efficient spattering of the Ge surface.

1. Introduction

Porous germanium (PGe), which for first time was experimentally discovered in the work [1], is now widely used in optoelectronics and to create solar cell elements [2] as in case of Si. There were developed various technologies for the creation of PGe layers, such as the electrochemical treatment of single-crystal *c*-Ge in highly concentrated electrolytes [3], plasma-stimulated chemical vapor deposition [4], spark discharge method [5], thermal annealing of GeO_2 ceramic films in a hydrogen atmosphere [6] and others.

A specific effective nonchemical technique for a fabrication of nanoscale thin PGe layers on the *c*-Ge surface is a high-dose implantation by various ions in a vacuum. The first direct evidence of the PGe formation by such technological approach was obtained by electron-microscopic observations, while *c*-Ge was irradiated by Ge^+-ions at energy of 50 keV [7]. Subsequently, the porous structure was recorded, as shown in the review [8], for as amorphous (a-Ge) and as *c*-Ge substrates by low-energy high-dose (>1 MeV) implantation with variety of ions: Ga^+, Ge^+, Mn^+, Ni^+, In^+, Sn^+, Sb^+, I^+, Au^+ and Bi^+. It should be mentioned some publications [9, 10] in which the Ag^+-ion implantation at high energies of 100 MeV, but rather small doses in the range of $5.0 \cdot 10^{12}$–$2.0 \cdot 10^{14}$ ion/cm^2, was used to create PGe layers and to produce their crystallization.

The present work is also devoted to the creation of PGe layers by the ion implantation method, but the general aim is to synthesize Ag nanoparticles simultaneously with the PGe structure (Ag:PGi). For this purpose, the low-energy (<100 keV) high-dose (>$1.0 \cdot 10^{17}$ ion/cm^2) Ag^+ -ion implantation of *c*-Ge was applied, similar to fabrication of porous Si layers with Ag nanoparticles by ion irradiation of c-Si [11, 12]. Interest in porous semiconductor structures with noble metal nanoparticles showing plasmon resonance properties is due to the prospects of their use in various applications: to increase the absorptivity in solar cells [13], to improve photoconductivity [14], to generate electron-hole pairs [15] and so on.

2. Experimental

Polished *c*-Ge substrate with thickness of 0.5 mm was used to obtain a structured surface Ag:PGe layer. For this purpose the implantation of *c*-Ge was carried out by Ag^+ ions with an energy of 30 keV at an irradiation dose of $1.5 \cdot 10^{17}$ ion/cm^2 and a current density of 5 μA/cm^2 with the ion accelerator ILU-3 at room temperature of the irradiated substrate. Observation of morphology of the sample surface and energy-dispersive X-ray (EDX) spectral microanalysis of implanted Ge was carried out with a high-

* Corresponding author. Kazan Physical-Technical Institute, RAS, 420029, Kazan, Russia.
E-mail address: aanstep@gmail.com (A.L. Stepanov).

https://doi.org/10.1016/j.vacuum.2018.03.030
0042-207X/

resolution scanning electron microscopes (SEM) SU 8000 (Hitachi) and Merlin Zeiss equipped by Aztec X-Max spectrometer (Oxford Instruments). Structure of surface sample layer was characterized by electron backscattered diffraction (EBSD) patterns using HKL NordLys detector (Oxford Instruments).

In a further experiment, in order to determine the appearance of a step due to sputtering or swelling of the surface at the boundary of the irradiated and unirradiated portions of the sample, a nickel mask with square mesh size 20 μm was superimposed on the *c*-Ge substrate surface during irradiation. Measurement of the step profile was carried out by the FastScan (Bruker) atomic force (AFM) microscope.

3. Results and discussion

Due to the peculiarities of ion implantation, the distribution of implanted ions in the irradiated material is not homogeneous in the depth of the sample. Therefore, using the computer program SRIM-2013 (www.srim.org) for modeling of profiles of implanted ions and generated vacancies in depth of irradiated matrices [16], the corresponding distributions for the case of Ag^+-ion implantation with en energy of 30 keV into Ge were calculated (Fig. 1 a, b). It is found that in the initial period of irradiation in the near-surface region of Ge there is an accumulation of silver atoms with a maximum of the statistical Gaussian concentration distribution in the sample depth is R_p ~14.6 nm, and the straggle of the ion range from R_p is ΔR_p ~6.9 nm (Fig. 1 a). The effective thickness of the implanted layer is estimated as $R_p + 2\Delta R_p = 28.4$ nm. However, as will be shown below, prolonged ion irradiation of *c*-Ge, simultaneously with the formation of PGe and the segregation of Ag at the sample surface, leads to an effective Ge sputtering. The profile of the generated vacancies in Ge during Ag^+-ion implantation has the same Gaussian shape and practically coincides with the distribution of Ag^+ ions in the depth of the sample (Fig. 1b).

SEM images of the Ge surface implanted with Ag^+ ions presented with various scales are shown in Fig. 2 and 3. Unlike the virgin polished *c*-Ge substrate (the right-hand side in Fig. 1b), the morphology of the irradiated surface is seen as the highly developed open porous spongy structure (Fig. 1a). Note that similar a spongy structure of PGe was formed by implantation of *c*-Ge, for example, by Bi^+-ion with an energy of 30 keV [8], but it is differs significantly from the columnar type PGe formed by implantation with a lighter Ge^+ ion at low energies [15, 17]. In principal, the possibility of creating pores by implantation with Ge^+ self-ions indicates that the formation of pores is happened not due the presence of an impurity, but because of some specific energy conditions during irradiation [18], which could be assumed also for our case Ag:PGi too, although heavy implants such as Ag could stimulate the appearance of a generally spongy structure.

The morphological homogeneity of the Ag: PGe surface observed over a large enough area of the sample in tens of microns (Fig. 2a) indicates that the porous structure is not a random local artifact of surface change during implantation, and could be characterized by the concept of scalability important for certain technological applications. EDX microanalysis of the implanted *c*-Ge surface is characterized by a spectrum with Ag peaks in the energy range of 2.5–3.5 keV (insert in Fig. 2a), which were not observed in the spectrum of unirradiated *c*-Ge. As the scale of the surface fragment increases (Figs. 2b and 3), a pore structure consisting of interlacing Ge nanowires (gray color) with average diameter sizes of about 10–20 nm could be seen more clearly. At the ends of Ge nanowires, close to spherical ion-synthesized nanofragments - nanoparticles (bright spots) with the sizes of ~20–30 nm are observed. For clarity, some of these nanoparticles are marked in Fig. 3a by circles. Since heavier chemical elements detected by the

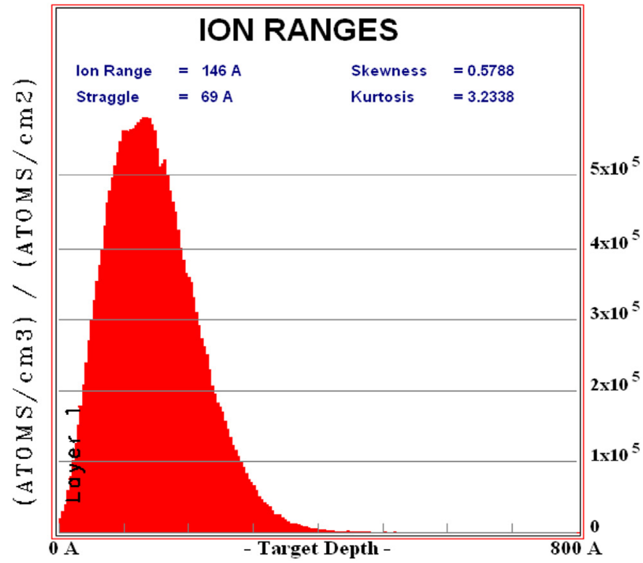

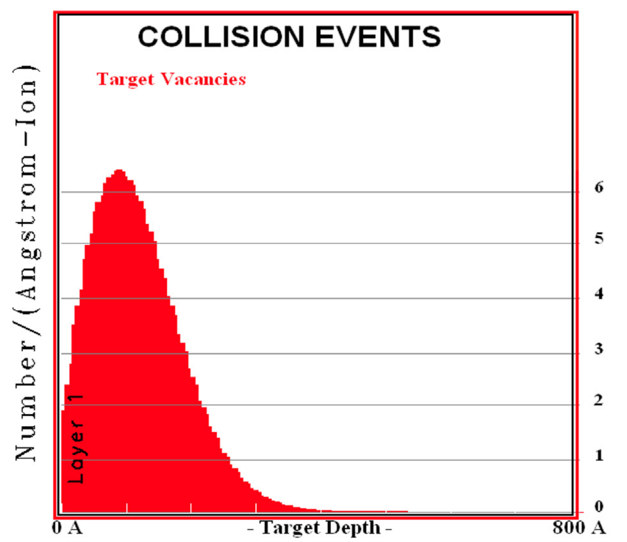

Fig. 1. Simulated depth distribution profiles of implanted Ag^+-ions (a) and generated vacancies (b) in irradiated Ge.

backscattered electron detector are shown in SEM images in a brighter tone color, for a composite material consisting only of Ge atoms and implanted Ag one, it can be assumed that the circled bright spots are determined as the ion-synthesized metallic Ag in the form of nanoparticles (Fig. 3a). It should be noted that the solubility of Ag in Ge is extremely small (~10^{16} at/cm^{-3}), and for the dose of $1.5 \cdot 10^{17}$ ion/cm^2 used in this study, by analogy with various implanted dielectrics [19], the generation of Ag nanoparticles in Ge is quite realistic. Herewith, atoms of Ag and Ge do not form any chemical compounds. A similar situation was observed earlier by SEM images for porous layers of PSi and PGeSi with Ag nanoparticles formed by the low-energy high-dose Ag^+-ions implantation [11, 12, 20].

The inset in Fig. 1b (on the right side) shows the experimentally observed EBSD picture of the Kikuchi diffraction from the virgin *c*-G. It means that the *c*-Ge substrate used in this work is characterized by a single-crystal cubic structure with the parameters a = b = c = 5.66 Å and $\alpha = \beta = \gamma = 90°$. For the implanted region of

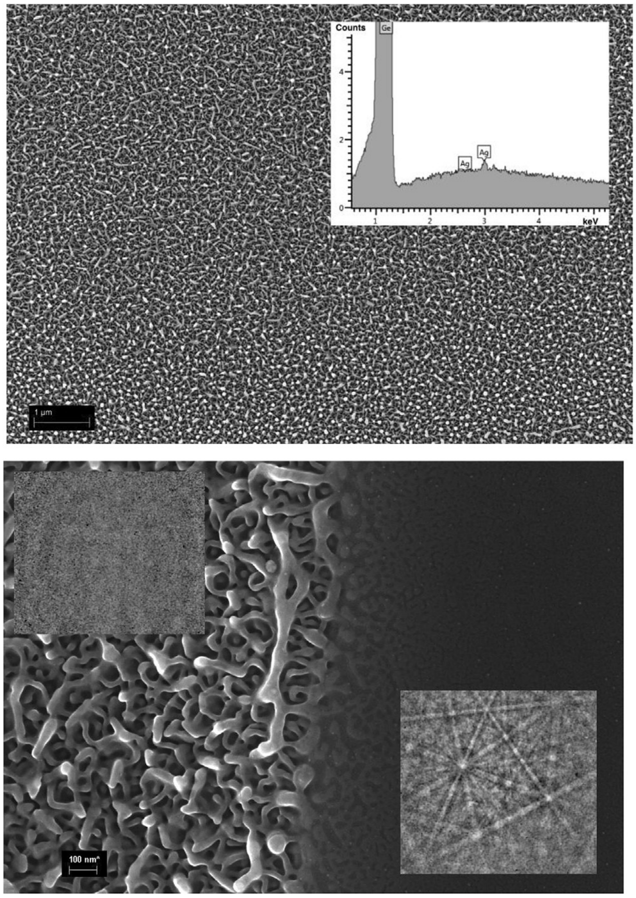

a

b

Fig. 2. SEM images, shown at different scales, of the Ag:PGe surface obtained by low-energy high-dose Ag^+-ion implantation into *c*-Ge. The inset in Fig. 2a shows the EDX spectrum. The right-hand side of Fig. 2b demonstrates the non-irradiated area of the virgin *c*-Ge substrate, and the left corresponds to implanted Ag:PGe region. Corresponding inserts are represented by the EBSD patterns.

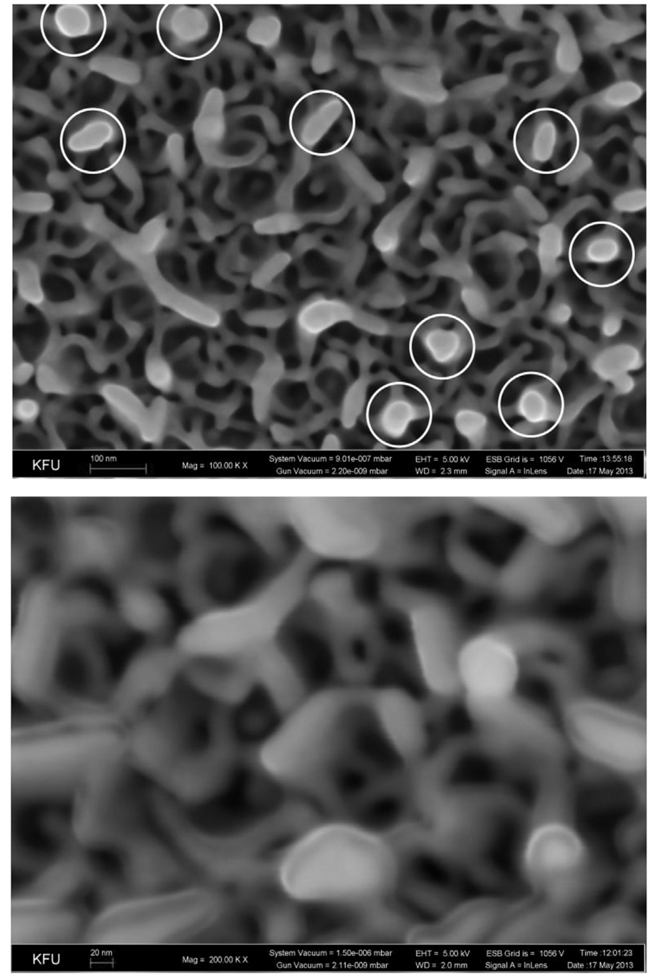

a

b

Fig. 3. SEM images, shown at different scales, of the Ag:PGe surface with ion-synthesized Ag nanoparticles.

the Ag:PGe sample, unlike the Kikuchi diffraction in the form of parallel lines to the planes of the crystal lattice bands, a EBSD pattern is observed from the wide diffuse rings (the insert on the left in Fig. 1b) of the amorphous layer PGe.

In order to evaluate the emerging step on the boundary between the irradiated and non-irradiated regions of a sample, due to sputtering or swelling of the surface, in particular when creating pores in semiconductors, for example, in case of Ge when irradiated with Ge^+ self-ion, implantation through a mask is traditionally used [17, 18, 21]. The SEM images of the Ge surface containing fragments of PGe microstructures formed by Ag^+-ion implantation through a mask are shown in Fig. 4. For the purpose of an independent evaluation of the topology of the surface after implantation, observations were made at different scales and with two different electron microscopes SU 8000 (Fig. 4a, c) and Merlin (Fig. 4b). As can be seen from these images, as a result of implantation on the *c*-Ge surface, square immersed areas of PGe are formed, bounded by the walls of the unirradiated c-Ge, which indicates the effective sputtering of the Ge surface, rather than its swelling. The SEM image, with a largest magnification at the corner of the square cell (Fig. 4c) clearly demonstrates the formation of spongy PGe in the implanted area of the cell.

A fragment of the sample, covering a region of several square mask cells, represented in the 3D projection of AFM image of an implanted Ag:PGe, is shown in Fig. 5. As seen from this figure, during the Ag^+-ion implantation of *c*-Ge simultaneously with the formation of the porous structure, an effective sputtering of the surface of the c-Ge substrate occurs, which confirms the SEM results (Fig. 4). In this case, a step on the boundary between *c*-Ge walls and sputtered PGe area are formed. According to the AFM profile measurement the depth of sputtering sample sections is estimated to be ~200 nm.

From the mass ratios of Ge and Ag atoms for case of low implantation energy (30 keV), it could be assumed that the nuclear collisions of Ag^+ ions with the substrate Ge atoms dominate, and as a result, the latter are sputtered by the direct knockout mechanism from the target [8, 18]. This fact is important from the point of view of determining the pathways for the formation of PGe, and it turns out to be somewhat unexpected, because of as it was previously shown the formation of pores in *c*-Ge implanted with Ge^+ self-ions was accompanied by the opposite phenomenon, surface swelling [17]. Therefore, the mechanism for the formation of pores in implanted *c*-Ge, based on the generation and unification of vacancies in an irradiated semiconductor, proposed for example in [8], could not be simply transferred to the case of implantation of c-Ge with heavy Ag^+ ions as in present study. It should be also mentioned that early it was shortly reported on appearance of PGe structure during Ag^+-ion implantation [22]. However, an information on a formation of Ag nanoparticles and Ag–PGe composition was not presented.

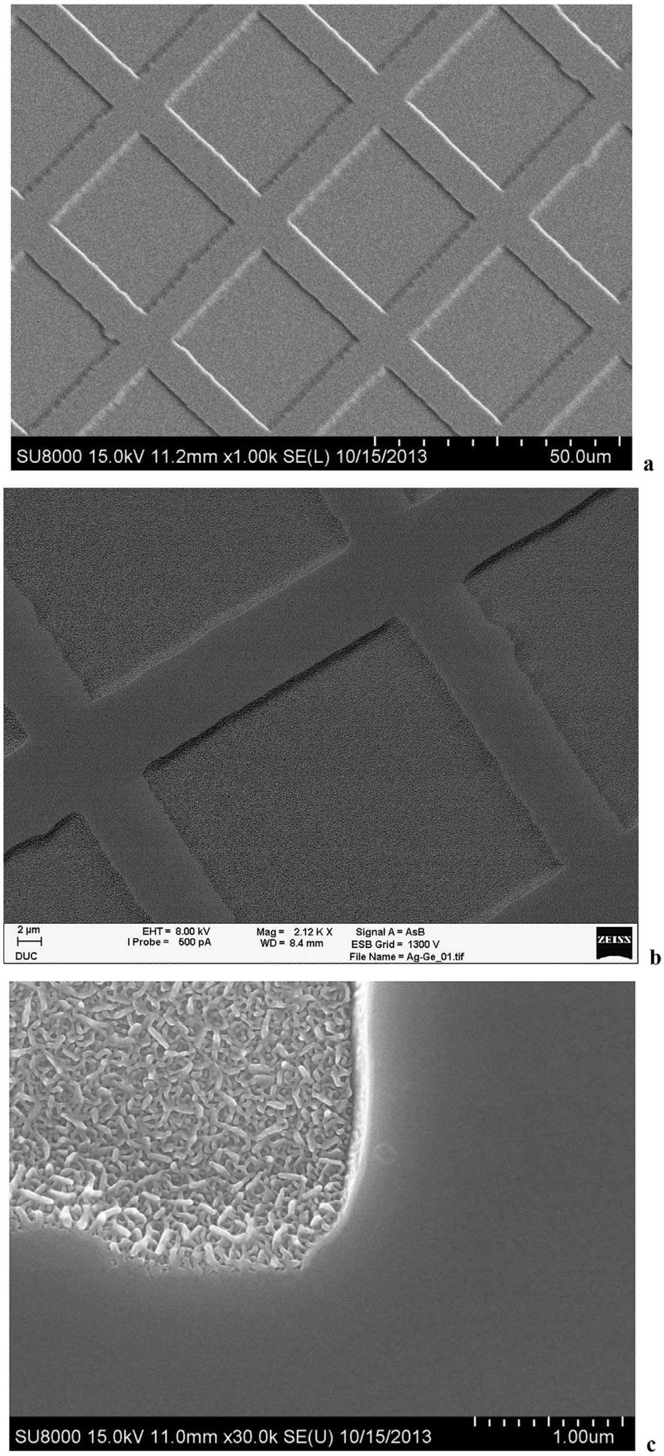

Fig. 4. SEM images, shown at different scales, of periodic microstructures on the *c*-Ge surface with PGe areas obtained by Ag^{+} ion implantation through a mask.

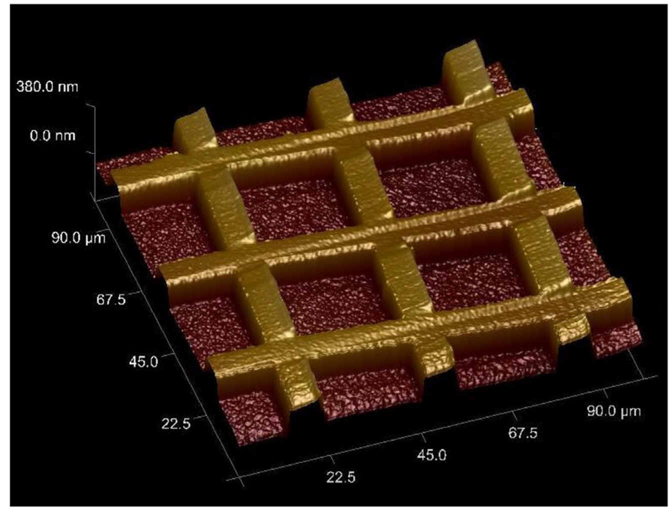

Fig. 5. 3D fragment of the AFM image of the *c*-Ge surface in the mask region, demonstrating Ge sputtering during implantation.

4. Conclusion

Thus, in this paper, for the first time a technique for obtaining PGe layers with Ag nanoparticles on the c-Ge surface using low-energy high-dose implantation was demonstrated. It was found that Ag^{+}-ion implantation leads to sputtering of the surface on which a spongy amorphous porous structure with metal nanoparticles is formed. Ion implantation technology is currently one of the main techniques used in industrial semiconductor microelectronics to form various types of Ge and GeSi nano- and micro-devices. Therefore, the considered suggested method of obtaining PGe by irradiation with Ag + ions, unlike chemical approaches, has the advantage in that it can be easily integrated into the modern industrial process of improving the technology of manufacturing microchips.

Acknowledgements

This work was supported by the Russian Science Foundation No. 17-12-01176.

References

[1] T.M. Donovan, K. Heinemann, Phys. Rev. Lett. 27 (1971) 1974–1976.
[2] E.G. Rojas, J. Hensen, J. Carstensen, H. Föll, R. Brendel, ESC Transactions 33 (2011) 95–102.
[3] G. Flamand, J. Poortmans, K. Dessein, Phys. Stat. Sol. C 2 (2005) 3243–3247.
[4] J. Shieh, H.L. Chen, T.S. Ko, H.C. Cheng, T.C. Chu, Adv. Mat 16 (2004) 1121–1124.
[5] G. Kartopu, S.C. Bayliss, R.E. Hummel, Y. Ekinci, J. Appl. Phys. 95 (2004) 3466–3472.
[6] C. Jing, C. Zhang, X. Zang, W. Zhou, W. Bai, T. Lin, J. Chu, Sci. Technol. Adv. Mater 10 (2009), 65001-1–65001–65006.
[7] I.H. Wilson, J. Appl. Phys. 53 (1082) (1698-1705).
[8] R. Böttger, K.-H. Heinig, L. Bischoff, B. Liedke, S. Facsko, Appl. Phys. A 113 (2013) 53–59.
[9] T. Som, J. Ghatak, O.P. Sinha, R. Sivakumar, D. Kanjilal, J. Appl. Phys. 103 (2008), 123532–1-123532-5.
[10] S. Hooda, S.A. Khan, B. Satpati, D. Strange, D. Buca, M. Bala, C. Pannu, D. Kanjilal, D. Kabiraj, Appl. Phys. A 122 (2016), 227-1–227–7.
[11] A.L. Stepanov, A.A. Trifonov, Y.N. Osin, V.F. Valeev, V.I. Optolectr, Adv. Mater. Rapid Comm 7 (2013) 692–697.
[12] A.L. Stepanov, V.I. Nuzhdin, V.F. Valeev, V.V. Vorobev, T.S. Kavetskyy, Y.N. Osin, Rev. Adv. Mater. Sci. 40 (2015) 155–164.
[13] A. Polman, Science 322 (2008) 868–869.
[14] H. Atwater, A. Polman, Nature Mat 9 (2010) 205–213.
[15] A. Cavalcoli, B. Fraboni, G. Impellizzeri, L. Romano, E. Scavetta, M.G. Grimaldi, Microporous and Mesoporous Mater 196 (2014) 175–178.
[16] J.F. Ziegler, J.P. Biersack, U. Littmark, The Stopping and Range of Ions in Solids, Pergamon Press, New York, 1985.
[17] L. Romano, G. Impellizzeri, M.V. Tomasello, F. Giannazzo, C. Spinella, M.G. Grimaldi, J. Appl. Phys. 107 (2010) 84314–84315, 84314-1–.
[18] S. Hooda, B. Satpati, S. Ojha, T. Kumar, D. Kanjilal, D. Kabiraj, Mater. Res. Exp 2

(2015), 45903–1-45903-10.
[19] A.L. Stepanov, R.A. Ganeev, A.I. Ryasnyansky, T. Usmanov, Nucl. Instr. Meth. Phys. Res. B 206 (2003) 624–628.
[20] R.I. Batalov, V.V. Vorobev, V.I. Nuzhdin, V.F. Valeev, R.M. Bayazitov, N.M. Lyadov, Y.N. Osin, A.L. Stepanov, Tech. Phys. 61 (2016) 1871–1877.
[21] W. Wesch, C.S. Schnohr, P. Kluth, Z.S. Hussain, L.L. Araujo, R. Giulian, D.J. Sprouster, A.P. Byrne, M.C. Ridgway, J. Phys. D: Appl. Phys. 42 (2009), 115402–1-115402-5.
[22] A.L. Stepanov, V.V. Vorobev, Y.N. Osin, M.A. Ermakov, V.F. Valeev, V.I. Nuzhdin, Sci. J. Microelectr 4 (2014) 11–17.